

## Magnetic domain pattern asymmetry in (Ga, Mn)As/(Ga, In)As with in-plane anisotropy

L. Herrera Diez, C. Rapp, W. Schoch, W. Limmer, C. Gourdon et al.

Citation: *J. Appl. Phys.* **111**, 083908 (2012); doi: 10.1063/1.4704385

View online: <http://dx.doi.org/10.1063/1.4704385>

View Table of Contents: <http://jap.aip.org/resource/1/JAPIAU/v111/i8>

Published by the [American Institute of Physics](#).

---

### Related Articles

Magnetically and thermally induced switching processes in hard magnets

*J. Appl. Phys.* **112**, 083919 (2012)

Spin-wave modes and band structure of rectangular CoFeB antidot lattices

*J. Appl. Phys.* **112**, 083921 (2012)

Perpendicular magnetic anisotropy in Nd-Co alloy films nanostructured by di-block copolymer templates

*J. Appl. Phys.* **112**, 083914 (2012)

Influence of microstructure and interfacial strain on the magnetic properties of epitaxial Mn<sub>3</sub>O<sub>4</sub>/La<sub>0.7</sub>Sr<sub>0.3</sub>MnO<sub>3</sub> layered-composite thin films

*J. Appl. Phys.* **112**, 083910 (2012)

Room temperature ferromagnetic behavior in cluster free, Co doped Y<sub>2</sub>O<sub>3</sub> dilute magnetic oxide films

*Appl. Phys. Lett.* **101**, 162403 (2012)

---

### Additional information on *J. Appl. Phys.*

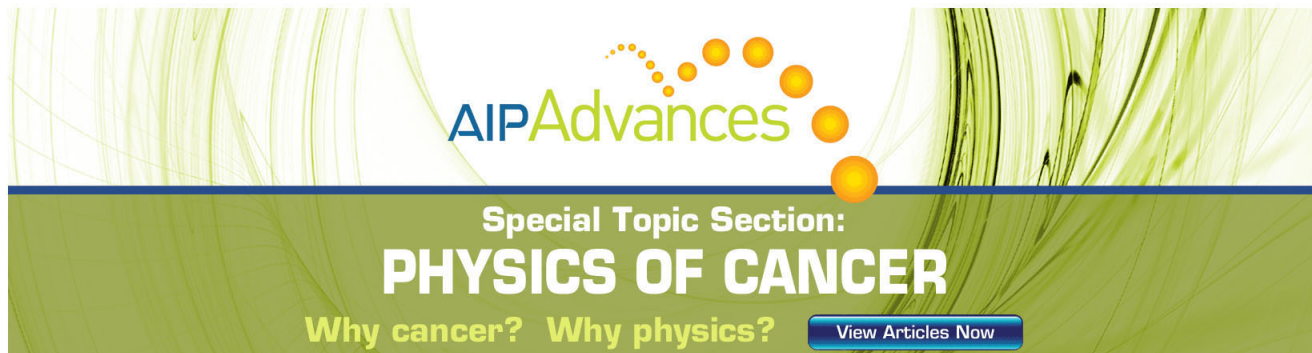
Journal Homepage: <http://jap.aip.org/>

Journal Information: [http://jap.aip.org/about/about\\_the\\_journal](http://jap.aip.org/about/about_the_journal)

Top downloads: [http://jap.aip.org/features/most\\_downloaded](http://jap.aip.org/features/most_downloaded)

Information for Authors: <http://jap.aip.org/authors>

## ADVERTISEMENT



**AIP Advances**

Special Topic Section:  
**PHYSICS OF CANCER**

Why cancer? Why physics? [View Articles Now](#)

## Magnetic domain pattern asymmetry in (Ga, Mn)As/(Ga,In)As with in-plane anisotropy

L. Herrera Diez,<sup>1,a)</sup> C. Rapp,<sup>2</sup> W. Schoch,<sup>2</sup> W. Limmer,<sup>2</sup> C. Gourdon,<sup>3</sup> V. Jeudy,<sup>4,5</sup>  
J. Honolka,<sup>1</sup> and K. Kern<sup>1</sup>

<sup>1</sup>Max-Planck-Institut für Festkörperforschung, Heisenbergstrasse 1, 70569 Stuttgart, Germany

<sup>2</sup>Institut für Quantenmaterie, Universität Ulm, D-89069 Ulm, Germany

<sup>3</sup>Institut des Nanosciences de Paris, UPMC, CNRS UMR 7588, 4 place Jussieu, 75005 Paris, France

<sup>4</sup>Laboratoire de Physique des Solides, Université Paris-Sud, CNRS, 91405 Orsay, France

<sup>5</sup>Université Cergy-Pontoise, 95000 Cergy-Pontoise, France

(Received 16 August 2011; accepted 16 March 2012; published online 18 April 2012)

Appropriate adjustment of the tensile strain in (Ga, Mn)As/(Ga,In)As films allows for the coexistence of in-plane magnetic anisotropy, typical of compressively strained (Ga, Mn)As/GaAs films, and the so-called cross-hatch dislocation pattern seeded at the (Ga,In)As/GaAs interface. Kerr microscopy reveals a close correlation between the in-plane magnetic domain and dislocation patterns, absent in compressively strained materials. Moreover, the magnetic domain pattern presents a strong asymmetry in the size and number of domains for applied fields along the easy  $[1\bar{1}0]$  and hard  $[110]$  directions which is attributed to different domain wall nucleation/propagation energies. This strong influence of the dislocation lines in the domain wall propagation/nucleation provides a lithography-free route to the effective trapping of domain walls in magneto-transport devices based on (Ga, Mn)As with in-plane anisotropy. © 2012 American Institute of Physics. [<http://dx.doi.org/10.1063/1.4704385>]

(Ga, Mn)As (Ref. 1) has demonstrated to be a good model system for the study of a number of magneto-electric properties with a marked potential for applications in spintronics. Among these properties, hole-mediated ferromagnetism<sup>2-4</sup> and strain-controlled magnetic anisotropy<sup>5-7</sup> stand out as the most promising and have been thoroughly investigated using a wide variety of device designs. The material growth parameters have shown to be of crucial importance for controlling these key magnetic and electrical properties in (Ga, Mn)As systems. One of the most prominent examples is the use of epitaxial buffer layers such as GaAs or (Ga,In)As to induce in-plane or perpendicular anisotropy, respectively. These procedures rely on the high sensitivity of (Ga, Mn)As magnetic anisotropy to compressive and tensile epitaxial strain.<sup>8-11</sup>

In this work, we present the study of the in-plane magnetic domain wall propagation/nucleation behaviour in (Ga, Mn)As/(Ga,In)As. The system studied combines in-plane magnetic anisotropy, typical of compressively strained materials, with the structural features of the tensile strained (Ga, Mn)As/(Ga,In)As. In order to realize the coexistence of these properties the material composition, given by the growth parameters, was set close to that of the transition from in-plane to perpendicular anisotropy. Magnetic imaging studies of (Ga, Mn)As/(Ga,In)As with in-plane or perpendicular anisotropy in the literature have been almost exclusively dedicated to the observation of the magnetization component perpendicular to the plane.<sup>12</sup> Therefore, it is interesting to perform a more detailed characterization of the in-plane magnetic domain

structure in (Ga, Mn)As/(Ga,In)As systems with in-plane anisotropy. In the following, we present the domain wall propagation/nucleation behaviour in (Ga, Mn)As/(Ga,In)As under in-plane magnetic fields. A marked asymmetry in the domain pattern is found for fields applied along the  $[110]$  and  $[1\bar{1}0]$  directions. The origin of this asymmetry is discussed in terms of direction dependent nucleation/propagation energies.

The (Ga, Mn)As/(Ga,In)As samples under study were grown by low-temperature molecular beam epitaxy and consist of a 180 nm thick (Ga, Mn)As film grown on a 3.5  $\mu\text{m}$  thick (Ga,In)As buffer layer. The Curie temperature and hole concentration are 66 K and  $3.6 \times 10^{20} \text{ cm}^{-3}$ , respectively. The Mn and In compositions are 5% and the growth temperatures of the magnetic and buffer layers are 250 °C and 430 °C, respectively. A more detailed description of the growth procedure can be found elsewhere.<sup>11</sup> For these samples, the lattice mismatch at the (Ga, Mn)As/(Ga,In)As interface induces a tensile stain of  $-0.08\%$  on the (Ga, Mn)As film accompanied by well known structural features. These features are multiple dislocations at the (Ga,In)As/GaAs interface that share the lattice misfit and form the so-called cross-hatch pattern.<sup>13</sup> The role of crystal defects and in particular of the cross-hatch pattern has been widely studied in connection with the magnetic domain pattern in ferromagnetic films.<sup>14,15</sup> In general, a domain wall pinning potential can build up at the dislocation lines<sup>16</sup> and consequently the magnetic domains arrange in patterns that resemble the crystalline defect structure. In (Ga, Mn)As/(Ga,In)As, the dislocations at the (Ga,In)As/GaAs interface give rise to undulations of the upper (Ga, Mn)As magnetic layer that have shown to strongly interact with the magnetic domain walls in films with perpendicular anisotropy.<sup>12,17</sup> The interaction between domain walls and surface undulations is evidenced as

<sup>a)</sup>Present address: Institut Néel – Département Nano, Equipe Micro et Nano Magnétisme, 25 Av. des Martyrs, Bât. K, 38042 Grenoble cedex 09, France. Electronic mail: [liza.herreradiez@grenoble.cnrs.fr](mailto:liza.herreradiez@grenoble.cnrs.fr).

a cross-hatched magnetic domain pattern and can be related to a strain modulation, and therefore a magnetic anisotropy modulation, that reflects the underlying dislocation pattern.<sup>12</sup>

Fig. 1 displays the calculated anisotropy energy landscape of the (Ga, Mn)As samples under study given by the dependence of the normalized free energy  $F_M(\mathbf{m})$  on the orientation  $\mathbf{m}$  of the magnetization  $M$  with respect to the crystalline axes. As shown in Fig. 1(a), the calculated energies have contributions from crystalline (tetragonal symmetry), shape, and in-plane uniaxial anisotropy. These contributions have different coefficients and dependencies on the projection of the magnetization vector on the crystalline axes. The values of the coefficients accounting for each anisotropy contribution are:  $B_{4\parallel} = -30$  mT,  $B_{4\perp} = -20$  mT,  $B_{001} = 15$  mT, and  $B_{1\bar{1}0} = -5$  mT for in-plane crystalline, out-of-plane crystalline, shape + uniaxial out-of-plane ( $m_z^2$  terms), and in-plane uniaxial anisotropy, respectively. It is worth noting that the magneto-elastic interactions in this system are contained in the values of  $B_{4\parallel}$ ,  $B_{4\perp}$ , and  $B_{2\perp}$  (the latter included in  $B_{001}$ ) which are strain dependent. The values of all the coefficients were obtained by the analysis of angle-dependent magneto-transport measurements performed at a temperature of 4 K (not shown). A detailed description of this procedure can be found in previous publications.<sup>11,18,19</sup> The plot of the total energy in Fig. 1(a) indicates that even in the presence of a tensile strain of  $-0.08\%$  provided by the (Ga,In)As buffer layer the out of plane axis remains a hard axis. Therefore, the magnetization is compelled to lie within the (001) plane. The energy contour along the (001) plane in Fig. 1(b) shows the in-plane anisotropy landscape given by the in-plane crystalline and uniaxial anisotropy components.

The energy barriers set by the magnetic anisotropy can, in general, be overcome by a high enough magnetic field. In this case, the in-plane anisotropy is rather weak since a modest magnetic field of 450 Oe perpendicular to the plane of the sample is enough to create domains, where the magnetiza-

tion aligns with the out-of-plane hard axis at a temperature of 4 K. The magnetic domain pattern obtained in this experiment is shown in Fig. 2. The interaction between surface undulations and the magnetic domain walls results in a characteristic cross-hatch domain pattern where well defined areas between strong pinning lines have different magnetization orientation. The polar Kerr microscopy image in Fig. 2 shows these differently magnetized regions as dark and bright areas. The dark areas indicate the regions where the magnetization aligns with the external perpendicular magnetic field. The bright areas indicate the parts where the magnetization still remains in the plane of the film. Similar magnetic imaging studies of the out-of-plane magnetization component in (Ga, Mn)As/(Ga,In)As with in-plane easy axes can be found in the literature and are in agreement with the Kerr microscopy image presented in Fig. 2.<sup>12</sup>

The same (Ga, Mn)As/(Ga,In)As system imaged in Fig. 2, patterned into Hall-Bar structures, was investigated under in-plane magnetic fields. In this case, longitudinal Kerr microscopy at 4 K provided the necessary magnetic contrast to visualize the in-plane magnetic domain pattern. The images in Fig. 3 correspond to the time evolution of the in-plane domain pattern in a constant magnetic field oriented at approximately  $10^\circ$  away from the  $[1\bar{1}0]$  uniaxial easy direction ((a) to (c)) and along the  $[110]$  hard direction ((d) to (e)). The constant magnetic field was applied after saturation in the opposite polarity (2000 Oe). The field values are 34 Oe and 25 Oe for the  $[1\bar{1}0]$  and  $[110]$  orientations, respectively. These values are the minimum needed for the appearance of reversed areas in the film for a waiting time of approximately 30 s after the application of the magnetic field, thus the system is in the thermally activated depinning regime. The times informed in Fig. 3 for each image ( $\Delta t$ ) are taken with reference to a time  $t_0$  (time zero) at which the first switched area is observed. It is important to notice that both orientations were measured in one and the same (Ga, Mn)As device.

Fig. 3 shows a clear asymmetry between the domain wall propagation/nucleation for the magnetic field applied

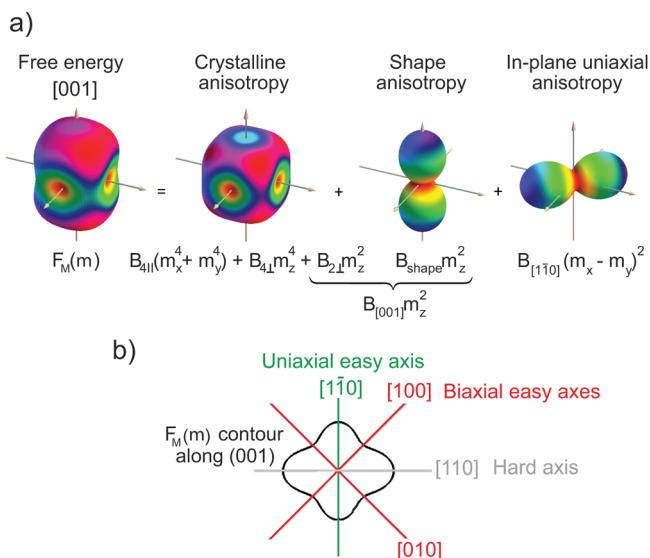


FIG. 1. (a) Total normalized free energy  $F_M(\mathbf{m})$  as a function of the magnetization direction. The calculation considers contributions from crystalline (tetragonal symmetry), shape, and in-plane uniaxial anisotropy. The easy axes lie in the plane of the sample for a tensile strain of  $-0.08\%$ , the energy contour line (b) shows the energy minima in the (001) plane.

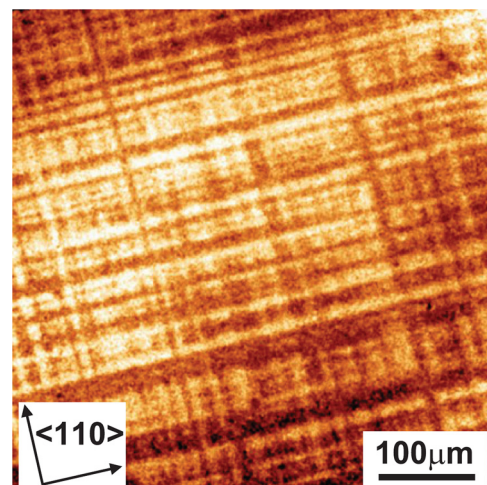


FIG. 2. Out-of-plane projection of the magnetization in a perpendicular field of 450 Oe at a temperature of 4 K. Dark areas indicate domains with perpendicular magnetization and bright areas domains with in-plane magnetization.

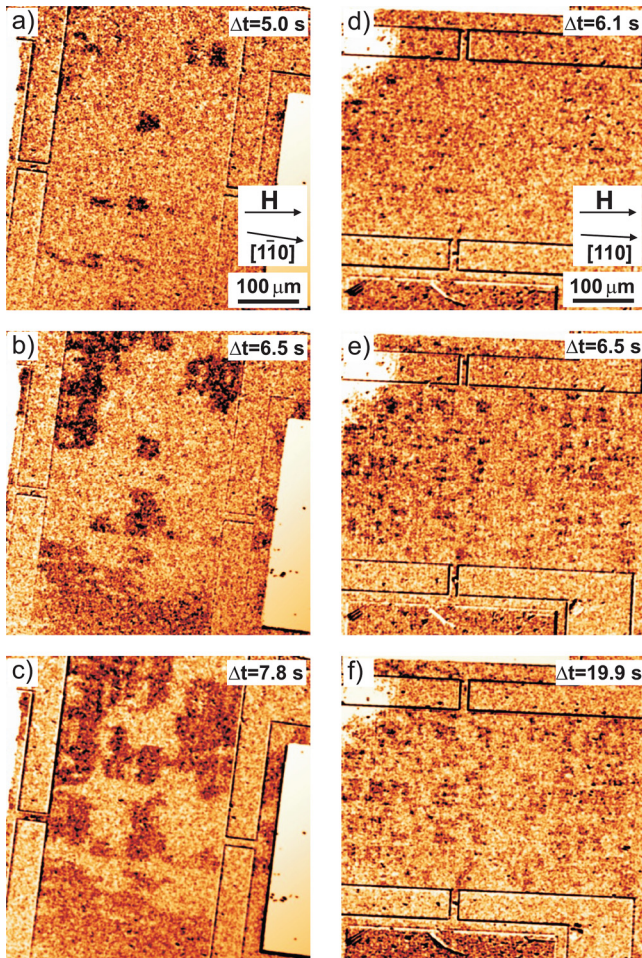


FIG. 3. Time evolution of the domain pattern at 4 K in a constant magnetic field oriented close to the uniaxial easy  $[1\bar{1}0]$  direction ((a) to (c)) and the hard  $[110]$  direction ((d) to (f)). The field values are 34 Oe and 25 Oe, respectively. The time  $\Delta t$  elapsed since time zero (the time at which the first switched area is observed) is indicated in each image.

along the  $[1\bar{1}0]$  uniaxial easy and  $[110]$  uniaxial hard directions. For the field applied close to the  $[1\bar{1}0]$  uniaxial easy direction, the domains are clearly defined by the position of the surface undulations (and underlying dislocation lines) known to be oriented along the  $[1\bar{1}0]$  and  $[110]$  directions.<sup>13</sup> This gives a domain pattern composed in its majority of domains with well defined square and rectangular shapes whose edges are aligned with the  $[1\bar{1}0]$  and  $[110]$  directions. When the field is applied along the uniaxial hard axis direction, the domain pattern shows a critical reduction in the size of the domains. In addition, the magnetic domains are significantly augmented in number with respect to the scenario for the field applied along the uniaxial easy direction.

As mentioned, due to the interaction between domain walls and surface undulations the domain pattern follows the underlying cross-hatched dislocation pattern which is identical for the field applied along the uniaxial easy and hard axis since all measurements were performed on the same device. This indicates that the reason for the asymmetry in the domain pattern may be a dependence of the domain wall pinning strength of the surface undulations on the direction of the applied magnetic field used to nucleate the magnetic domains. A similar asymmetry was shown in previous publications only

in compressively strained (Ga, Mn)As/GaAs films,<sup>21</sup> in the absence of the cross-hatch dislocation pattern. The cited work shows how the direction of the applied magnetic field can dramatically affect the domain wall dynamics. Going from the uniaxial easy to the uniaxial hard axis, the domain wall dynamics changes from a propagation dominated to a nucleation dominated scenario, respectively. In addition, the estimation of the nucleation/propagation energies from angle resolved coercivity measurements reveals the existence of different types of domain walls for the two different field directions. These two domain wall types (in this case  $60^\circ$  and  $120^\circ$  domain walls) given by the interplay between in-plane crystalline and uniaxial anisotropy have different values of the estimated nucleation/propagation energies explaining the observed differences in the domain wall dynamics behaviour.

In view of these facts, it is likely that the in-plane domain nucleation/propagation behaviour in tensile strained (Ga, Mn)As/(Ga,In)As shares a similar scenario with the compressively strained (Ga, Mn)As/GaAs materials. Different domain wall types maybe generated for fields applied along and perpendicular to the  $[110]$  direction, giving rise to different interactions with the surface undulations. A possible explanation could be given by a larger pinning efficiency of the undulations for domain walls generated under fields applied along the  $[110]$  hard direction. Within this framework, the system would evolve as a large collection of small domains where domain wall propagation is largely impeded and the reversal is driven by multiple domain nucleation. On the other hand, the domain walls generated with fields along the uniaxial easy direction may still have a strong interaction with the surface undulations but smaller than that of the previous case. Consequently, the domain walls are able to overcome pinning energy barriers that were active for domain walls generated with fields along the uniaxial hard axis. This would determine that the reversal along the  $[1\bar{1}0]$  direction is slightly more propagation dominated than that of the  $[110]$  direction showing a smaller quantity of larger domains rather than a large amount of small domains. This interpretation, derived from results reported on compressively strained (Ga, Mn)As/GaAs systems may be a reasonable scenario for the domain wall propagation/nucleation behaviour in tensile strained (Ga, Mn)As/(Ga,In)As with in-plane anisotropy.

It is worth discussing at this point the known asymmetry in the dislocation distribution that can be found at the (In,Ga)As/GaAs interface in relation with the magnetic domain patterns presented earlier. Studies in the literature identify an anisotropic distribution of dislocations along the  $[1\bar{1}0]$  and  $[110]$  directions for (Ga,In)As/GaAs (Ref. 20) and also in (Ga, Mn)As/(Ga,In)As (Ref. 12) films. The asymmetry is caused by the unequal number of  $\alpha$  and  $\beta$  dislocation lines along the two  $\langle 110 \rangle$  perpendicular directions. The  $\alpha$  and  $\beta$  dislocation types differ in their core structure and in their dynamic and electronic properties. Assuming that the interaction of a magnetic domain wall with a surface undulation could depend on the structure of the  $\alpha$  and  $\beta$  underlying dislocations, this would only lead to an anisotropic domain wall propagation. Namely, if the wall has a stronger interaction with the undulations produced by one of the dislocation types, the propagation along the crystalline direction that is rich in this dislocation

type would be largely impeded with respect to the perpendicular direction. This would lead to domains that grow preferentially along the direction with the least number of strongly interacting undulations, regardless of the direction of the applied field. In the case presented in this work, the domain wall propagation does not show a preferential direction. Therefore, the presence of an anisotropic  $\alpha$  and  $\beta$  dislocation distribution cannot be the origin of the observations presented.

In conclusion, we have shown the close correlation between the cross-hatch dislocation pattern and the in-plane magnetic domain pattern in tensile strained (Ga, Mn)As/(Ga, In)As materials. A strong asymmetry in the size and number of magnetic domains has been identified for applied fields along and perpendicular to the in-plane uniaxial easy axis. By analogy with compressively strained materials, we propose this asymmetry to be linked to the generation of different domain wall types upon changing the direction of the applied field. This different domain wall types would generate different interactions with the surface undulations generated by dislocations at the (Ga, In)As/GaAs interface giving rise to the observed asymmetry in the domain wall propagation/nucleation behaviour.

It is important to note that the observed strong correlation between the dislocation lines and the magnetic domain pattern may be used as a lithography-free route to the effective trapping of domain walls in magneto-transport devices based on (Ga, Mn)As with in-plane anisotropy. For devices of reduced dimensions, the dislocation lines can generate surface undulations that cross the entire width of the device providing well defined regions of opposite magnetization that can be used for the study of single defect depinning processes as done in other materials such as FePt.<sup>22</sup> Additionally, it is known that magnetic domain walls in (Ga, Mn)As with in-plane anisotropy have a rather complex alignment with respect to the crystal-line axes.<sup>23</sup> Therefore, the presence of pinning lines along crystalline directions provides a natural way of obtaining aligned domain walls for applications, where the defined orientation of flat domain walls is required, such as in current-induced domain wall motion experiments.

- <sup>1</sup>H. Ohno, *Science* **281**, 951 (1998).
- <sup>2</sup>T. Dietl, H. Ohno, and F. Matsukura, *Phys. Rev. B* **63**, 195205 (2001).
- <sup>3</sup>D. Chiba, M. Sawicki, Y. Nishitani, Y. Nakatani, F. Matsukura, and H. Ohno, *Nature (London)* **455**, 515 (2008).
- <sup>4</sup>I. Stolichnov, S. W. E. Riester, H. J. Trodahl, N. Setter, A. W. Rushforth, K. W. Edmonds, R. P. Campion, C. T. Foxon, B. L. Gallagher, and T. Jungwirth, *Nature Mater.* **7**, 264 (2008).
- <sup>5</sup>A. W. Rushforth, E. De Ranieri, J. Zemen, J. Wunderlich, K. W. Edmonds, C. S. King, E. Ahmad, R. P. Campion, C. T. Foxon, B. L. Gallagher, K. Výborný, J. Kučera, and T. Jungwirth, *Phys. Rev. B* **78**, 085314 (2008).
- <sup>6</sup>C. Bihler, M. Althammer, A. Brandlmaier, S. Geprägs, M. Weiler, M. Opel, W. Schoch, W. Limmer, R. Gross, M. S. Brandt, and S. T. B. Goennenwein, *Phys. Rev. B* **78**, 045203 (2008).
- <sup>7</sup>M. Overby, A. Chernyshov, L. P. Rokhinson, X. Liu, and J. K. Furdyna, *Appl. Phys. Lett.* **92**, 192501 (2008).
- <sup>8</sup>T. Jungwirth, J. Sinova, J. Maek, J. Kučera, and A. H. Mac-Donald, *Rev. Mod. Phys.* **78**, 809 (2006), and references therein.
- <sup>9</sup>A. Shen, H. Ohno, F. Matsukura, Y. Sugawara, N. Akiba, T. Kuroiwa, A. Oiwa, A. Endo, S. Katsumoto, and Y. Iye, *J. Cryst. Growth* **175–176**, 1069 (1997).
- <sup>10</sup>L. Thevenard, L. Largeau, O. Manguin, G. Patriarche, A. Lemaître, N. Vernier, and J. Ferré, *Phys. Rev. B* **73**, 195331 (2006).
- <sup>11</sup>M. Glunk, J. Daeubler, L. Dreher, S. Schwaiger, W. Schoch, R. Sauer, W. Limmer, A. Brandlmaier, S. T. B. Goennenwein, C. Bihler, and M. S. Brandt, *Phys. Rev. B* **79**, 195206 (2009).
- <sup>12</sup>A. Dourlat, V. Jeudy, C. Testelin, F. Bernardot, K. Khazen, C. Gourdon, L. Thevenard, L. Largeau, O. Manguin, and A. Lemaître, *J. App. Phys.* **102**, 023913 (2007).
- <sup>13</sup>K. H. Chang, P. K. Bhattacharya, and R. Gibala, *J. Appl. Phys.* **66**, 2993 (1989).
- <sup>14</sup>R. Ranjan, O. Buck, and R. B. Thompson, *J. Appl. Phys.* **61**, 3196 (1987).
- <sup>15</sup>S. Tsukahara and H. Kawakatsu, *J. Phys. Soc. Jpn.* **21**, 313 (1966).
- <sup>16</sup>L. Schultz, *J. Magn. Magn. Mater.* **13**, 251 (1979).
- <sup>17</sup>K. Y. Wang, A. W. Rushforth, V. A. Grant, R. P. Campion, K. W. Edmonds, C. R. Staddon, C. T. Foxon, B. L. Gallagher, J. Wunderlich, and D. A. Williams, *J. Appl. Phys.* **101**, 106101 (2007).
- <sup>18</sup>W. Limmer, M. Glunk, J. Daeubler, T. Hummel, W. Schoch, R. Sauer, C. Bihler, H. Huebl, M. S. Brandt, and S. T. B. Goennenwein, *Phys. Rev. B* **74**, 205205 (2006).
- <sup>19</sup>W. Limmer, J. Daeubler, L. Dreher, M. Glunk, W. Schoch, S. Schwaiger, and R. Sauer, *Phys. Rev. B* **77**, 205210 (2008).
- <sup>20</sup>O. Yastrubchak, T. Wosiński, J. Z. Domagała, E. Łusakowska, T. Figiel-ski, B. Pécz, and A. L. Tóth, *J. Phys.: Condens. Matter* **16**, S1S8 (2004).
- <sup>21</sup>L. Herrera Diez, R. K. Kremer, A. Enders, M. Rössle, E. Arac, J. Honolka, K. Kern, E. Placidi, and F. Arciprete, *Phys. Rev. B* **78**, 155310 (2008).
- <sup>22</sup>J. P. Attané, D. Ravelosona, A. Marty, Y. Samson, and C. Chappert, *Phys. Rev. Lett.* **96**, 147204 (2006).
- <sup>23</sup>J. Honolka, L. Herrera Diez, R. K. Kremer, K. Kern, E. Placidi, and F. Arciprete, *New J. Phys.* **12**, 093022 (2010).